JACOBS PUBLISHERS

OPEN ACCESS

Jacobs Journal of Enzymology and Enzyme Engineering

Research Article

Structural Characterization and Enzymatic Activity of the Recombinant Ala^{959} To Ser^{1066} Region of Human Ace

Caroline Cristina Eliasa[1], Larissa Miranda Pereira[1,2], Danielle S. Aragão[2], Dulce E. Casarini[2], Regina Affonso[1*]

[1]*Centro de Biotecnologia, Instituto de Pesquisas Energéticas e Nucleares, São Paulo, Brazil*

[2]*Departamento de Medicina, Disciplina de Nefrologia, Universidade Federal de São Paulo, Escola Paulista de Medicina, São Paulo, Brazil*

[1]*These authors contributed equally to the work*

**Corresponding author:* *Dr. Regina Affonso, Biotechnology Center, IPEN-CNEN, Av. Prof. Lineu Prestes, 2242, Cidade Universitária, 05508-000, São Paulo, Brazil. Tel: 55 21 11 31339707; E-mail: reginaffonso@yahoo.com.br*

Received: *11-10-2016*

Accepted: *03-06-2017*

Published: *28-06-2017*

Abstract

Angiotensin-converting enzyme catalyzes the conversion of angiotensin I to the vasoconstrictor angiotensin II and the hydrolysis of bradykinin (BK). Human somatic angiotensin-converting enzyme has two homologous domains (N and C) that share 60% identity. Although these two regions have high homology, the catalytic site of the C-domain exhibits three-fold greater activity than the N-domain in the hydrolysis of angiotensin I *in vivo*. The present study aimed to obtain the Ala^{959} to Ser^{1066} catalytic region of the C-domain of angiotensin-converting enzyme in a structural conformation that resembles its native form. We amplified the 324-bp sequence corresponding to the catalytic site of C-domain of angiotensin-converting enzyme and cloned this sequence into a pET28 vector. The catalytic site of C-domain of angiotensin-converting enzyme peptide was expressed in a bacterial system, and its purification was performed in one step using a His-tag affinity column. Structural analysis by circular dichroism and fluorescence confirmed that the purified protein is correctly folded, and catalytic site of C-domain of angiotensin-converting enzyme possesses enzymatic activity and is inhibited by lisinopril. This peptide can be used to test new inhibitors and C-domain of angiotensin-converting enzyme substrates because this peptide is easy to produce and this has proven efficient link with these molecules.

Keywords: Zinc Catalytic Site of sACEC; Recombinant Protein; Correct Structure; Enzymatic Activity

Introduction

Angiotensin-converting enzyme I (ACE) is a membrane-bound, zinc-dependent dipeptidase that catalyzes the conversion of angiotensin I to the potent vasopressor angiotensin II. ACE is a key part of the renin-angiotensin system, which regulates blood pressure and is widely distributed throughout the body [1].

There are two isoforms of human ACE, including the somatic ACE (sACE) present in somatic tissue and the testicular ACE (tACE) present in male germinal cells (Figure 1a). The tACE isoform is similar to the C-domain of sACE [2]. The sACE isoform possesses two catalytic sites which exhibit 60% sequence identity but catalyze the cleavage of angiotensin I and bradykinin with different efficiencies. The C-domain is the main catalyst responsible for angiotensin conversion in the body and the regulation of blood pressure. The N-domain is typically associated with the metabolism of biologically active peptides [3]. The two domains differ in terms of chloride-ion activation profiles, rates of peptide hydrolysis, and sensitivities to various inhibitors [1]. A more detailed analysis shows that these regions are composed of HEMGH and EAIGD sequences that bind zinc ions to facilitate catalytic activity, Figure 1a [4].

Extensive research over the past 30 years has been achieved

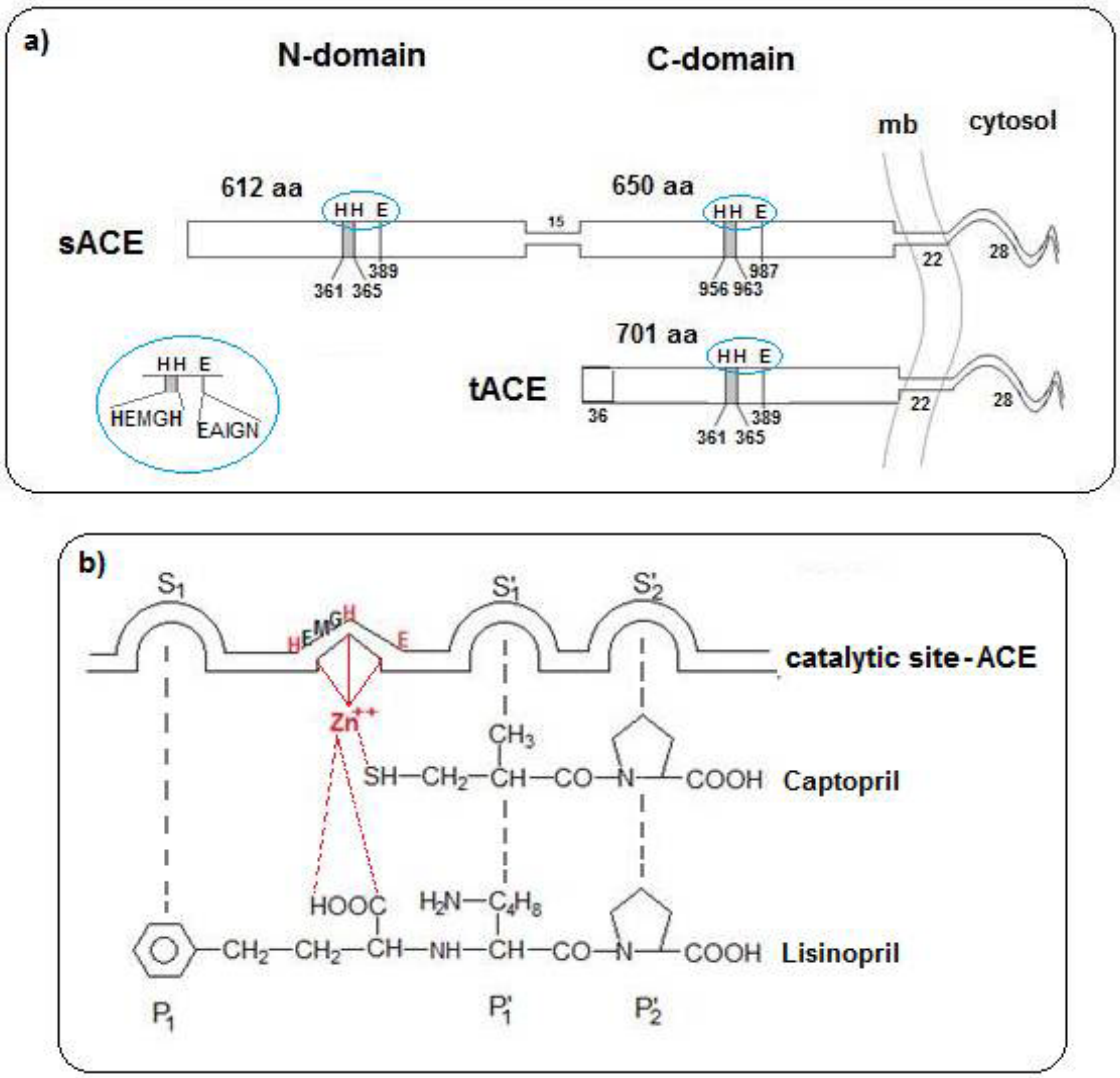

Figure 1. a) Schematic of the primary structural domains of somatic and testicular ACE. The cytoplasmatic region spans 28 aa, the C-terminal membrane anchor consists of 22 aa, and the locations of the active-site zinc-binding motif id indicated by HEMGH and EAIGN, in detail in the lower left corner – blue circle (modified from various authors, and the sequences numbers were obtained from Acharya et al. [4]).

b) Schematic of the ACE active site showing the relationships between the substrate sites (s_1, s'_1 and s'_2) and inhibitors (p_1, p'_1 and p'_2), dashed gray lines. The red lines represent the binding between Zn^{2+} and the catalytic site HEMGH and E, and the dashed red lines represent the binding between Zn^{2+} and specific inhibitor regions, captopril or lisinopril (modified from various authors).

Abbreviations: aACE, somatic angiotensin-converting enzyme; tACE, testicular angiotensin-converting enzyme; mb, cytoplasmic membrane; aa, amino acids; H, histindine; E, glutamic acid; M, methionine; G, glycine.

through the pioneering inhibitor studies of Ferreira et al., [5] and Ondetti et al. [6]. These researchers showed that the venom of a Brazilian pit viper contains a factor that greatly enhances the smooth muscle relaxation caused by the nonapeptide bradykinin and inhibits ACE [7].

Synthetic ACE inhibitors, such as captopril, have been used for more than 30 years in medicine. Currently, there are many commercial inhibitors, including benazepril, enalapril, fosinopril, and lisinopril. Inhibitors that are commonly used to study sACE binding include captopril, lisinopril and enalapril. The striking difference between these inhibitors is that coordination with zinc occurs at a sulfhydryl group of captopril and a carboxyl group in lisinopril, Figure 1b. Captopril interactions with the protein are held in place at only two additional positions: P_1'~S_1' and P_2'~S_2'. In contrast, interactions between lisinopril and the ACE occur at three positions: P_1~S_1, P_1'~S_1' and P_2'~S_2' [2].

Many studies investigated the conformational features that influence ACE catalytic activity. These studies often begin with the solid-phase synthesis of a 36-residue peptide that contains the amino acid composition and sequence of the ACE active-site fragment. This ACE active-site fragment is the zinc-binding sequence which comprises a fragment that contains three proposed protein binders, these are His361/959, His365/963 and Glu389/987, these correspond the two zinc binding sites: HEMGH and EAIGD (somatic isoform numbering; N- and C- domains, respectively), Figure 1a [7-10]. The synthetic form of this ACE peptide provides very important information about data as: correct sequence, structure, modeling, conformational and binding with zinc analysis [7,11]. Moreover, the use trifluoroacetic acid (TFA) or trifluoroethanol (TFE) can reduce the pH of a peptide preparation, and thus may alter the pH of subsequent assays, especially the activity assays [12].

Protein expression in the bacterium *E. coli* has been the most popular means of producing recombinant proteins for over three decades. *E. coli* is a well-established host that offers short culturing time, easy genetic manipulation and low cost media [13,14]. Additionally, *E. coli* has a long history of being able to produce a wide variety of different types of proteins [14]. Vamvakas et al. [9,10], produced the ACE peptide in the *E. coli* expression system with production in inclusion bodies. The ACE peptide after the purification it was refolded with TFE, which prevents the activity assay.

In a similar strategy, our current study obtained the Ala^{959} to Ser^{1066} catalytic region of the C-domain of sACE (sACEC) in a structural conformation that more closely resembles the native fold. Expression of this region was performed in soluble form and in a bacterial system. The final product possessed the expected α-helix and β-strand structure, bound zinc ions, cleaved the Hippuryl-His-Leu (Hip-His-Leu) substrate, and its enzymatic activity was inhibited by lisinopril.

Materials and Methods

Cloning and Expression of the Recombinant Protein

The cDNA of the human zinc catalytic site of cs-ACE_C was amplified from a pcDNA3.1-sACE construct (the plasmid was kindly provided by Dr. Pierre Corvol from the Institut National de la Santé et de la Recherche Médicale, College de France, Paris, France). The amplification was completed using PCR with the *Taq* polymerase enzyme and the following primers: forward NC 5' catgccatggcctcggcctgggac 3' (the restriction site NcoI is underlined) and reverse C 5' ggaattcgctgaaggggataaagg 3' (the restriction site EcoRI is underlined). The following PCR conditions were used: 95°C for 1:30 min, 30 cycles of 95°C for 15 sec, 55°C for 15 sec and 72°C for 15 sec (Taq polymerase, Ludwig Biotec, Brazil). The pET28a vector (Novagen, Darmstadt, Germany) and cDNA were digested using NcoI and EcoRI restriction enzymes (Thermo Scientific, Massachusetts, USA). Next, the digested products were ligated (T4 DNA Ligase, Ludwig Biotec, Brazil) and the product was cloned into *E. coli* BL21. The transformed *E. coli* BL21 culture containing the pET28cs-ACE_C plasmid was grown in LB medium (10 g/L tryptone, 5 g/L yeast extract, 10 g/L NaCl) supplemented with kanamycin (50 μg/mL) at 37°C while shaking at 180 rpm. When the OD_{600} reached 0.4-0.8, protein expression was induced with 0.5 mM isopropyl-β-D-thiogalactoside-IPTG (Ludwig Biotec, Brazil) [15], and expression cultures were incubated for 5 h and 16 h at 37°C with shaking at 180 rpm. The cultures were then centrifuged at 1,750 x g for 10 min at 4°C, and the pellets were processed or stored at -20°C [16].

cs-ACE_C Protein Isolation

All of the pellets were processed using the same protocol. The pellet from the induced culture was resuspended in 20 mM Tris-HCl and 100 mM NaCl buffer, pH 7.5. The suspension was sonicated seven times for 30 s on ice and centrifuged at 9,500 x g for 10 min at 4°C. The supernatant was stored on ice in 0.1 mM phenylmethylsulfonyl fluoride-PMSF (Sigma-Aldrich, Missouri, USA). The induced culture and supernatant were analyzed via sodium dodecyl sulfate polyacrylamide gel electrophoresis (SDS-PAGE) [17].

SDS-PAGE and Dot Blotting Analyzes

The *E. coli* samples transformed with pET28cs-ACE_C were cultured with different lengths of induction. Samples of: induced cultures, supernatants of the induced culture after of the centrifugation, purification and concentrated were analyzed by SDS-PAGE using a 15% denaturing polyacrylamide gel [17]. The gels were stained with Coomassie blue (Sigma-Aldrich, Missouri, USA). For dot blotting analyzes, the samples were dropped onto a nitrocellulose membrane (20 μL). The membrane was incubated with polyclonal goat anti-ACE_C antiserum (Abcam, UK) at a 1:500 dilution and then incubated with horseradish-peroxidase- conjugated anti-goat IgG (1:5000 dilution). An ECL Advance Western Blotting Detection Kit (GE) was used for visualization [15].

Protein Purification

The expressed cs-ACE_C was purified from the induced culture using immobilized metal-ion affinity (His Trap FF, General Eletric, USA) with an AKTA Protein Purification System (General Eletric, USA). The elution buffer contained 20 mM Tris-HCl, 100 mM NaCl and 0.5 M imidazole, pH 7.5. Linear and step gradients were used for elution with flow of 1 mL/min/fraction. The purification samples were analyzed via SDS-PAGE and dot blotting.

Protein Quantification

The protein concentration of the samples containing 6.0 M guanidine hydrochloride (Sigma-Aldrich, Missouri, USA) was determined by measuring the absorbance at 280 nm. The equation used for measuring the concentration of a protein in solution using absorbance spectroscopy is $A = \varepsilon^{x} L^{x} c$, where A is the absorbance, ε is the molar absorption coefficient, l is the sample-cell path length and c is the molar concentration of the sample (according to the Beer-Lambert Law [18]). The absorbance was measured using a NanoDrop 2000 spectrometer (Thermo Scientific, Massachusetts, USA).

Circular Dichroism (CD) Spectroscopy

After purification of cs-ACE_C, protein samples were concentrated and dialyzed against a 20 mM Tris-HCl and 100 mM NaCl buffer, pH 7.5, to remove imidazole. Next, samples (1.8 μM) were analyzed by circular dichroism. Far-ultraviolet CD spectra were obtained with a Jasco J-810 (Hachioji, Tokyo, Japan) spectropolarimeter using a 0.1-cm light path at 20°C. The ellipticity was recorded from 200 to 260 nm, and the scan was repeated four times. The signals from reference samples without protein were always subtracted. Temperature-dependent far-ultraviolet CD spectra analysis of cs-ACE_C was carried out in the same aforementioned buffer over a temperature range of 20°C to 90°C. The temperature was controlled using a Peltier-type TPC-423S/L Jasco temperature-control system (Hachioji, Tokyo, Japan), and the heating rate used was 5 or 10°C/min. Profiles were obtained using the program CDNN [19].

Fluorescence Spectroscopic Analyses

The tertiary structure of the cs-ACE_C protein (1.8 μM) was analyzed. The data were obtained for wavelengths ranging from 308 to 430 nm in an AB2 Luminescence Spectrometer (Thermo Scientific, Massachusetts, USA). Analyses of Zn^{2+} ion incorporation were conducted with 50 μM $ZnCl_2$ and a 30 minute incubation period at 25°C [16].

Enzymatic Activity Awssay

The cs-ACE_C activity was measured fluorimetrically using Hippuryl-His-Leu (Hip-His-Leu) as a substrate, as described by Friedland and Silverstein [20]. A sample of cs-ACE_C (50 μL – 1.8 μM) was incubated with 200 μL of assay solution containing 5 mmol/L Hip-His-Leu in 100 mmol/L potassium phosphate buffer, pH 8.3, 300 mmol/L NaCl and 0.1 mmol/L $ZnSO_4$ for 18 h at 37°C. The enzymatic reaction was stopped by the addition of 1.5 mL of 280 mmol/L NaOH. The solution was then incubated with 100 μL o-phthaldialdehyde (20 mg/mL in methanol) for 10 min. The fluorescent reaction was stopped by the addition of 200 μL 3 N HCl. The liberated dipeptide His-Leu was measured fluorimetrically (excitation 360 nm, emission 500 nm) using a Hitachi fluorimeter (Hitachi, Tokyo, Japan). To measure lisinopril inhibition, cs-ACEC was pre-incubated with the inhibitors for 30 min at 37°C. Next, Hip-His-Leu was added, and the aforementioned protocol was completed [21,22]. The standard curve was obtained using varying concentrations of L-His-Leu (0 – 5.5 mM) in the blank reaction mixture. The standard curve obtained showed a linear relation between relative fluorescence and His-Leu concentration [21].

Results

Cloning and Expression of Recombinant cs-ACE_C

Catalytic site expression was first performed using the p1813cs-ACE_C vector because this vector has been shown to produce 376 mg of hRPL10 protein per liter of induced bacterial culture [16]. However, the cs-ACE_C protein did not express well under the induction conditions. As a result, the pET28a vector was used because this vector contains a histidine sequence that is useful in purification. The cloning product was confirmed with sequencing (data not shown).

The expression of pET28cs-ACE_C was determined by incubating cultures at 37°C for 5 h and 16 h with 0.5 mM of IPTG. Next, the cultures were centrifuged, and the pellets were resuspended and sonicated. The supernatant of the sonicated pellet contained the protein of interest in a soluble form. After activation, the bacterial culture absorbance was approximately 1.0 unit, and the expression of the protein of interest was low. To solve this problem, we increased the volume of the expression culture to 0.8 L and extended the expression time.

Several reviews on *E. coli* production systems suggest that an increase in the production of recombinant protein may occur with increased expression times [23,24]. In this study, we cultivated *E. coli* at reduced temperatures at 18^0C, 25^0C and 30^0C with shaking of 150 rpm for 16 h [16]; however, cs-ACE_C showed very low production (data not shown).

Purification of cs-ACE_C Protein

The supernatants obtained after sonicating the induced cultures (5 h and 16 h) were analyzed by Ni-IMAC affinity chromatography using a His Trap column. For purification, the cs-ACE_C protein was eluted with 180 mM of imidazole buffer in a linear gradient; however, the protein eluted with many bacterial contaminants. The strategy used to purify the protein involved a step gradient, in which the protein was eluted in 100 mM of imidazole buffer. After purification, the samples were analyzed using SDS-PAGE. Figure 2a shows the 5 h samples, and 2b shows the 16 h samples. As shown in Figure 2b, high-molecular weight contaminants were observed in all purification samples eluted. In contrast, the cs-ACE_C sample shown in lane 3 of Figure 2a was pure.

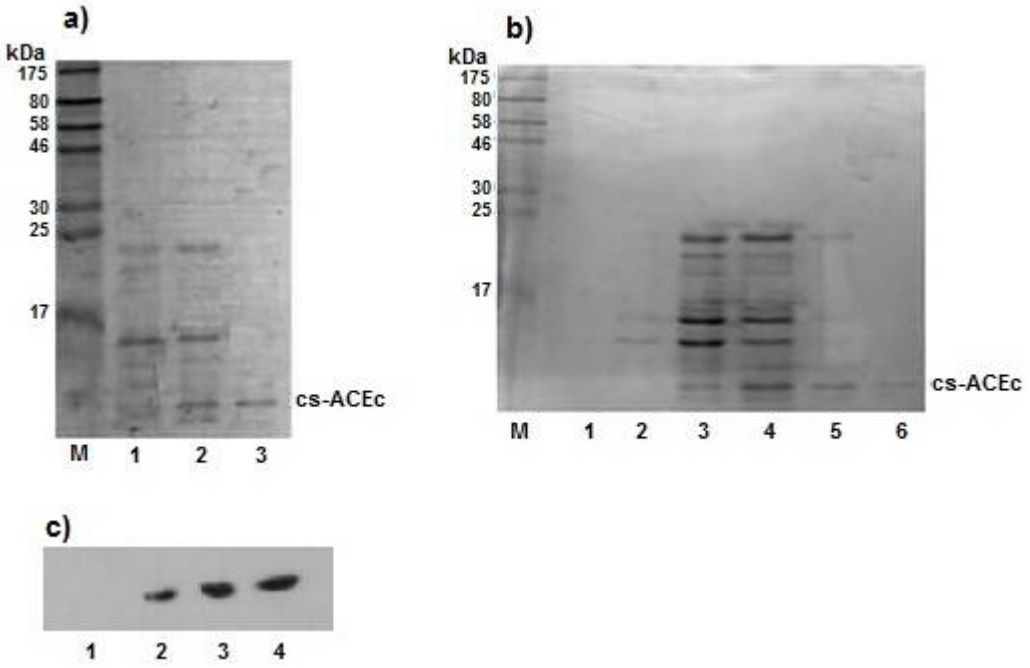

Figure 2. Analysis of cs-ACEc by SDS-PAGE and blotting

Analysis of cs- ACEc samples expressed in cultures of p ET28-csACEc-transformed *E.coli*. Culture were induced for 5 h (a, c) and 16 h (b) at 37^0C using 0.5 mM of IPTG and cs-ACEc was purified by immobilized metal-ion affinity- His Trap FF of 1 mL. SDS-PAGE:

a) Lane M, protein molecular weight; lane 1, culture induced; line 2, sup ematant after of the centrifugation of the sample 1; line 3, fractions eluted with 20% imidazole step (100mM).

b) Lane M, protein molecular weight; lane 1, culture non induced; line 2, culture induced 1; line 3, sup ematant after of the centrifugation of the sample 2; line 4 to 6, fractions eluted by linear gradient.

Dot blotting c) Lane 1, culture non induced; line 2, culture induced; line 3, purified and concentrated sample; line 4, mouse mesangial cells as positive control.

Our SDS-PAGE results showed that cs-ACE_C had an expected molecular weight of 12 kDa. Figure 2a (lanes 2 and 3) and Figure 2b (lane 4, 5 and 6) show a protein with a molecular weight between 10 and 15 kDa. Dot blotting immunological assay confirmed the identity of the protein as cs-ACE_C in the samples, Figure 2c.

cs-ACE_C Quantification

The quantification was determined by absorbance of 280 nm. The data used in the Beer-Lambert Law calculation included an ε = 0.77 and *l* = 1 mm (*web.expasy.org/protparam*). The results show that the concentration of pure cs-ACE_C was 2.3 mg of protein per liter of induced bacterial culture, after the purification. However, the total of cs-ACE_C protein expressed was 5 mg per liter of induced bacterial culture, this result was obtained with the culture of 5h, whereas for the culture of 16 h was lower.

Circular Dichroism Spectroscopy (CD) Analyses

The purified cs-ACE_C sample was concentrated and dialyzed to remove imidazole because this reagent causes problems in CD and fluorescence measurements [25]. The CD analysis was used to confirm the presence of secondary structures in the recombinant protein, which presented well-defined minimum peaks at 208 nm and 222 nm, Figure 3a.

Table 1 contains the percentages obtained in the CD analysis. The protein consisted of 76.7% alpha helices and 14.9% beta-strands. These data suggest that the protein has the correct structure. Our structure-based sequence comparison with the tACE catalytic site region and these regions were aligned [26], Figure 4a. In this figure there are three alpha helices long (α15, α17 and α19) and two small beta sheets only, this confirms our results data.

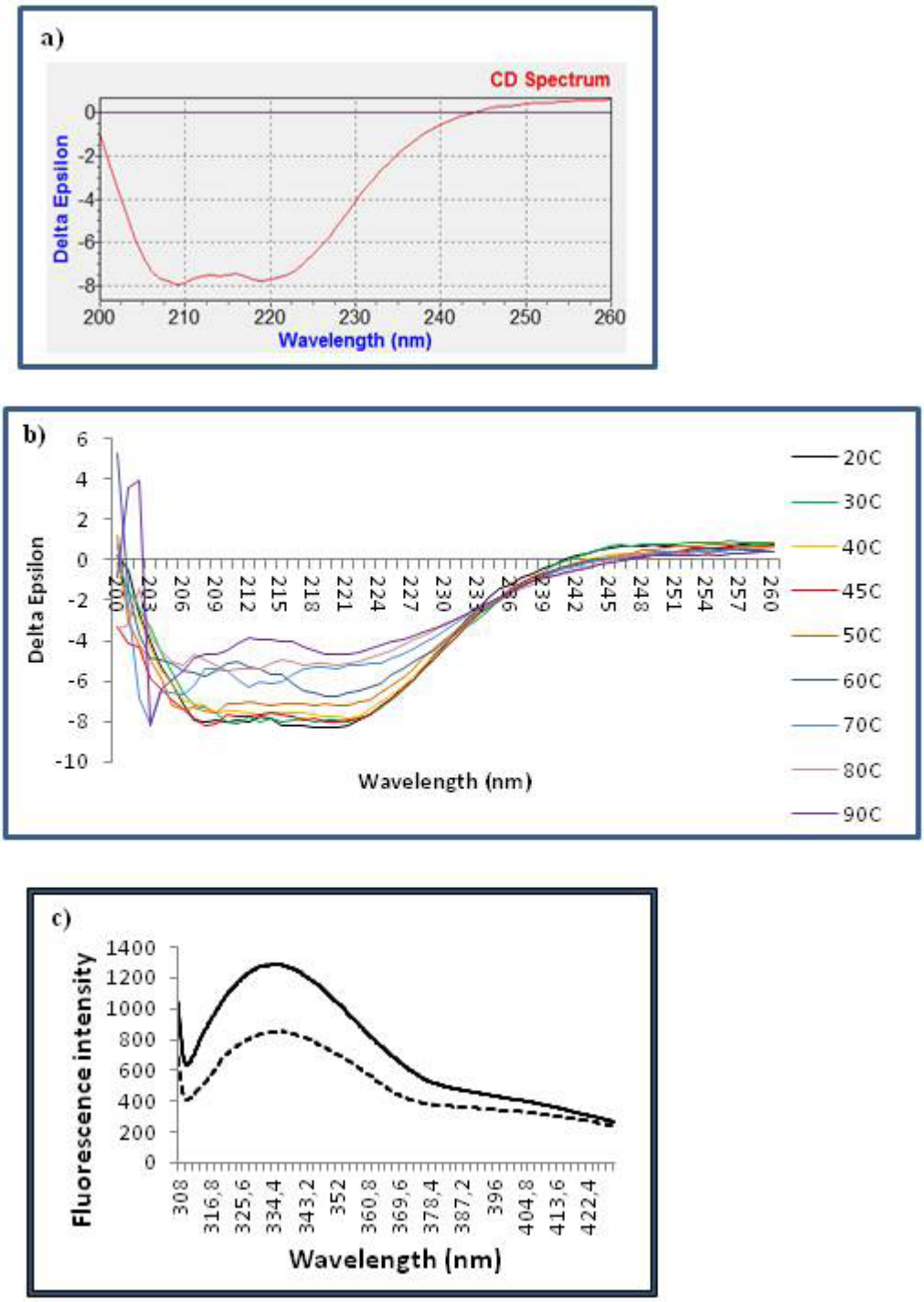

Figure 3. Circular dichroism analysis of the secondary structure of cs-ACEc (1.8 μM).

a) The data were obtained at 200c, and the profile was obtained with CDNN software.

b) The structure of cs-ACEc was analyzed at temperature ranging from 20^0c to 90^0c.

c) Fluorescene emission spectral analysis of the cs-ACEc protein (1.8 μM).

The spectra corresponding to Zn ion incorporation into the cs-ACEc protein: solid line, 0 μM $ZnCl_2$ and dashed line, 50 μM $ZnCl_2$

CD is a good tool to assess the conformation loss associated with a temperature increase. In this work, this analysis was applied to the cs-ACE_C protein. The CD data obtained for cs-ACE_C under different temperatures are shown in Figure 3b. The profiles were obtained at temperatures ranging from 20°C to 90°C. We observed a strong alteration in the 60°C profile. The CD data shown in Table 2 were analyzed using the CDNN program. We found that there was an increase in the random coil percentage at 60°C (9.8% to 14.6% at 50°C and 60°C, respectively). At these same temperatures there was a significant increase in β-strands from 15.6% to 18.4%.

c-ECA	α-Helix (%)	β-Sheet (%)	β-Turn (%)	Random Coil (%)
Expressed for 5 h	76.7	4.1	10.8	9.2

Table 1. Percentage of secondary structural elements in cs-ACE_C. The data were obtained at 20°C. The spectra were fitted using standard CDNN software. (available at http://bioinformatik.biochemetech.uni-halle.de/cd spec/cdnn).
The values obtained using this software can deviate between 5% and 10%.

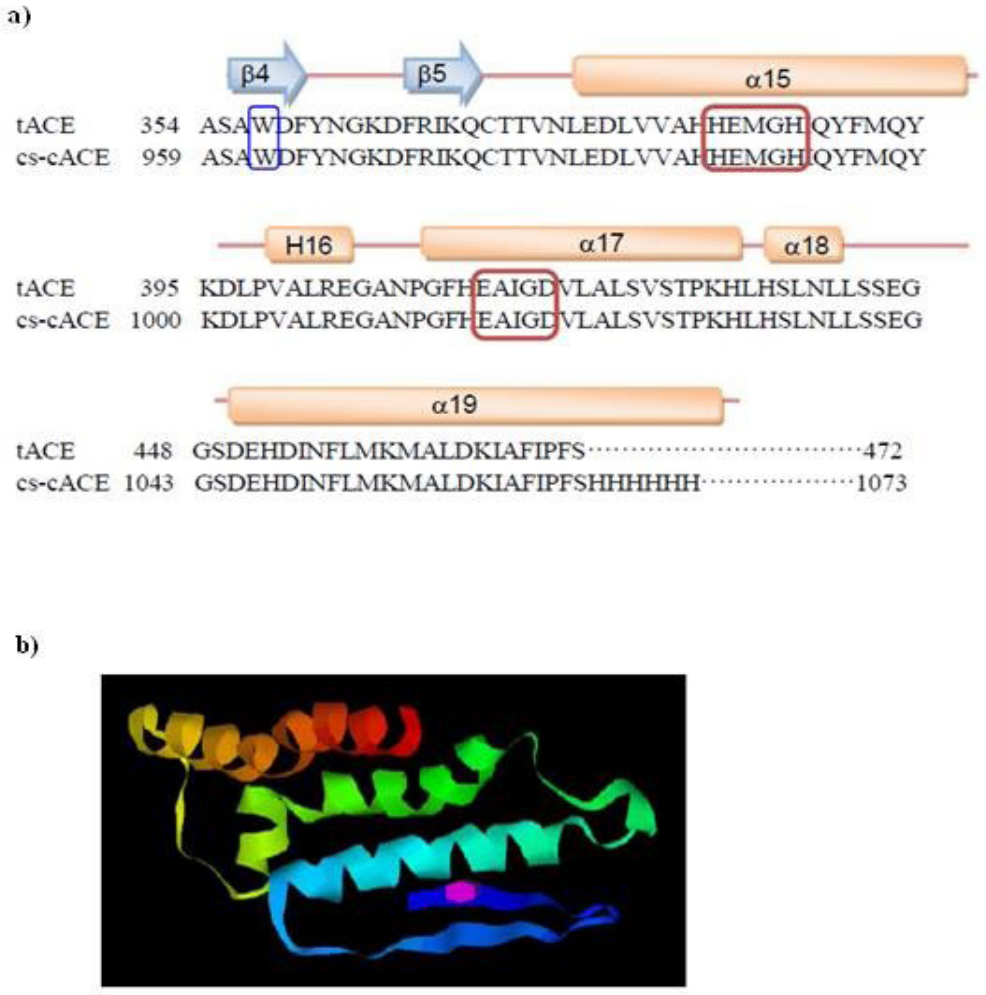

Figure 4. Schematic of the putative secondary and tertiary structures of cs-ACEc.

a) Alignment of the amino acids of tACE and cs-ACEc. The Zn-binding sites HEMGH in α15 and EAIGD in α17 are depicted in red, and the tryptophan residue in β4 is depicted in blue (modified from Corradi et al. [26]).

b) Illustration of the tertiary structure of the cs-ACEc protein. The tryptophan residue is shown in pink (RasMol software).

c-ECA	α-Helix	β-Sheet	β-Turn	Random Coil
	(%)	(%)	(%)	(%)
30°C	78.1	3.8	10.4	9.3
40°C	76.1	4.3	10.8	9.7
50°C	74.7	4.4	11.2	9.8
60°C	65.9	6.3	12.1	14.6
70°C	65.2	6.8	12.5	16
80°C	56.9	8.8	13.3	20.4
90°C	45.8	11.9	14.8	25.7

Table 2. CD data of cs-ACEC at various temperatures using CDNN software.

The values obtained using this software can deviate between 5% and 10%.

Fluorescence Spectroscopy Analyses

The tertiary structure of cs-ACE$_C$ was evaluated using fluorescence spectroscopy (Figure 3c). The cs-ACE$_C$ sequence contains one tryptophan (W) and six tyrosine (Y) residues and exhibited a maximum intrinsic fluorescence at 280 nm and an emission peak red-shifted to 335.4 nm (Figure 3c, solid line). ACE active sites possess the characteristic HEXXH zinc-binding motif, and the two His residues comprise the first two zinc ligands sites [11]. The third zinc ligand site, glutamic acid, is situated 23 residues toward the C-domain in the second characteristic sequence, EAXGD [7]. The fourth zinc ligand site is a water molecule [11]. The sequence analyzed in our work contains three zinc-binding residues, including His 988, His 992 and Glu 1016. Zinc is essential for catalytic site function, and the chemical shift perturbation mapping observed by Spyroulias et al. [7] proved that addition of the Zn ion in peptide solutions induced structural changes. The amino acids identified with potential zinc ligands are located in HEMGH and EAIGD sequences, and these two regions are localized in the two central α-helices (Figure. 4a, α15 and α17, respectively).
The zinc binding of cs-ACE$_C$ was assessed by the addition of $ZnCl_2$, which causes a change in the tryptophan spectroscopic properties, Fig 3c, dashed line. Specifically, fluorescence spectroscopic analysis of cs-ACE$_C$ with bound zinc ions revealed the displacement of the tryptophan maximum emission from 335.4 to 336.4 nm. This coincided with a significant decrease in intensity (from 1287.3 to 855).

cs-ACE$_C$ Activity

After confirmation of structure and zinc binding, we analyzed the enzyme activity of cs-ACE$_C$. The activity of cs-ACE$_C$ was inferred by measuring the degradation of the natural substrate molecule, Hip-His-Leu. This molecule was used in a Michaelis complex simulation. The cs-ACE$_C$ specific activity obtained was 20.4 ± 1.5 nM/min.

The K_M value obtained for cs-ACE$_C$ was 2.4 mM with the Hip-His-Leu substrate (Figure 5a).

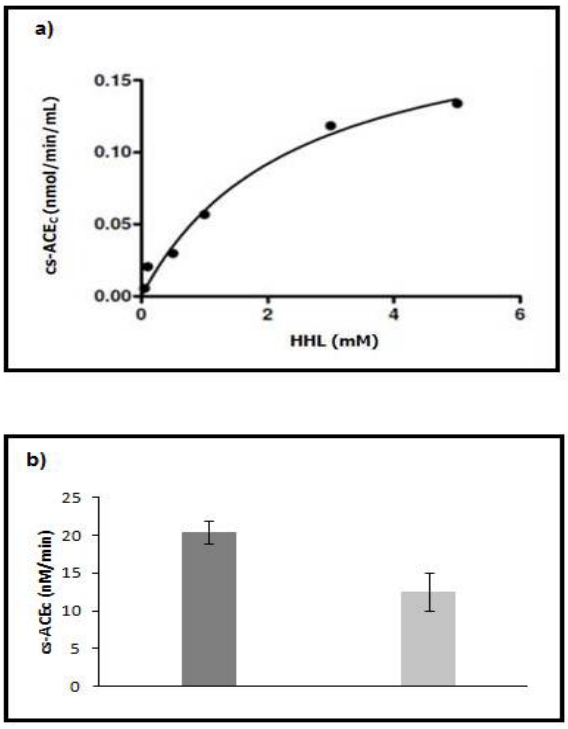

Figure 5. Activity assay of cs-ACEc (1.8 µM).

a) K_M cs-ACEc profile for the hydrolysis of the Hip-His-Leu (HHL) substrate (0 – 5.5 mM) (n=3).

b) Measurement of cs-ACEc activity using the Hip-His-Leu (5 mM) (grey) and cs-ACEc + lisinopril (0.1 µM) (light grey) (n=3).

Studies on the inhibition activity of ACEs show that there is a trend in the relative potencies of lisinopril, enalaprilat and captopril for the C-domain (L > E > C) [27]. This trend correlates with the number of interactions observed in the crystal structure complexes with tACE [28].

In the present work, we measured the activity of cs-ACE$_C$ in the presence of lisinopril, which owns a *Ki* six times less than the obtained with captopril, to C-domains [27]. We demonstrated that the addition this inhibitor resulted in lower activity, Fig-

ure 5b. The inhibition percentage was approximately 59% after lisinopril addition, 12.4 ± 2.5 nM/min.

Discussion

Antihypertensive drugs, in addition to their main activities, exhibit beneficial lateral effects on the prevention of cardiovascular disease, heart failure, post-myocardial infarction and diabetic nephropathy in various classes of hypertensive patients [22]. Expanding on previous studies of inhibitor activity, our work focused on the production of the recombinant zinc catalytic site of the C-domain of sACE in its active form.

In the literature, the catalytic site of sACE, N- and C- domain, were described its production in recombinant form or synthesized, and their conformational structures analyzed by CD and Nuclear Magnetic Resonance. However, these peptides did not have your activity evaluated. In present work, the cDNA to cs-ACE_C peptide was cloned, and its expression in bacterial system was of 5.0 mg per liter of culture. The concentration of the peptide pure and soluble was 2.3 mg per liter of culture, which was induced for 5h. This concentration was approximately half of the total production of the peptide. Vamvakas et al. [9,10] obtained 12 mg of the N-catalytic site and 6 mg of the C-catalytic site per liter of induced bacterial culture after purification. We believe that despite the pET28 to be of the same series as pET3, the cs-ACE_C total production was about 5 mg of protein per liter of induced bacterial culture, almost the same obtained by these authors [9]. However, the expression of this protein in soluble form enables completion of the solubilization/purification steps without the need for refolding.

Pereira et al. [16] had success obtaining soluble hRPL10 protein with decrease of bacterial growth temperatures. In the present work, the use of different temperatures did not contribute to increase the soluble forma of the cs-ACE_C. Extended activation times decrease the available oxygen in the cultures and increase the protein contaminants in the sample due to the expression of more than 200 genes related to the metabolic capacities of the cell [24]. A longer period of expression produced the same quantity of cs-ACE_C, but it also produced more contaminants. This result may be due to the production of more bacterial proteins over the course of 16 h [13,24].

Vamvakas et al. [10] proposed a different strategy for expression of cs-ACE_C. The authors expressed the protein in a pET3 vector in inclusion bodies, and solubilization and refolding were performed using a chemotropic agent and TFE, respectively. Chaotropic agents promote the disaggregation of the inclusion bodies; however, removal may cause aggregation or misfolding [29]. These authors used TFE to obtain the α helix conformation and then they could not make the enzymatic assay. Pereira et al. [16] demonstrated that inclusion bodies are formed by a tangle of soluble and aggregated protein; and we solved this problem by using a different expression vector, which expressed the csACEC in inclusion bodies, and the soluble form was isolated successful.

The CD analysis was vital for determining the secondary structure of recombinant cs-ACE_C protein. Previous studies created the catalytic sites of ACEN and ACEC by synthesizing and folding the protein constructs with TFA or TFE to promote helix formation. Spyroulas et al., [7] and Spyranti et al., [11] synthesized ACE catalytic site with a length of 36 aa and 37 aa, respectively. The region is composed only of an α-helix; thus, the use of TFE was to promote the native conformation because TFE has the ability to promote structure formation in peptide skeletons with high helix propensity. In the study with ACEN, Spyranti et al. [11] reported a 57% α-helix structure using 67% TFE. Vamvakas et al. [10] obtained a 41.1% α-helix structure using the maximum TFE concentration of 80%, with the same amino acids sequence of our work. Although TFE promotes the formation of α-helices, previous studies have reported lower percentages structure in α-helices, in peptide only formed by this structure, these measures could not be representing the real structure of the peptide.These results contradictory can be by the fact that the folding of certain proteins can form transient structures of non-native helices; this formation was described by Ikeguchi [28] with β-lactoglobulin. While β-lactoglobulin is a predominantly β-sheet protein, the protein has been shown to form non-native helices in early stages of folding with TFE. The presence of TFE or TFA could cause the formation of only α-helixes in the ACE peptide, which could compromise of subsequent CD analyzes. Finally, TFA/TFE can reduce the pH of a peptide preparation to ~2 to 3, thus may alter the pH of subsequent assays, and undertake experiments as the activity of pH 8.3 [12]. The cs-ACE_C construct consists of amino acid residues 959 to 1066 in the sequence. These amino acids are arranged in four alpha helices (α15, α17, α18 and α19), one 3_{10} short helix (H16) and two antiparallel β-strands (β4 and β5), Fig. 4a. In this figure, the alpha helices and β-strands position are as described in the work Corradi et al. [26] and it confirmed with RasMol software analysis. Therefore, we expressed cs-ACE_C in soluble form to ensure correct folding.

Analyses by circular dichroism collected as a function of temperature were made to determine the thermodynamics of protein unfolding. The data suggest that a significant change occurred in the cs-ACE_C structure at this temperature range because the β-strands are more exposed. Andrade et al. [1] detected significant alterations in the conformation of all rat ACE isoforms with the loss of α-helix structure at temperatures ranging from 40°C to 50°C, and the loss of structure was followed by the loss of activity. Analyses using temperature scanning of bovine ACE observed that the denaturation temperatures of the N- and C-domains were 55.3°C and 70.5°C, respectively [31]. These previous studies corroborate our results.

Fluorescence spectroscopy is widely used to study the structure of proteins and the dynamic properties that are directly related to their biological functions, such as specific binding [32]. Zinc is essential for catalytic site function, and the chemical shift perturbation mapping observed by Spyroulias et al. [7] proved that addition of the Zn ion in peptide solutions induced structural changes. The amino acids identified with potential zinc ligands are located in HEMGH and EAIGD sequences, and these two regions are localized in the two central α-helices (Figure 4a, α15 and α17, respectively).

Spyroulias et al. [7] analyzed the 36-residue peptide structure (from the HMEGH to the EAIG site) that contains the two zinc-binding motifs. This peptide contains only α-helixes. The authors observed that minor conformational differences between the free and zinc-bound peptides could be identified by changes in the secondary structure of the first binding motif (constituting the first pentapeptide fragment). The conformational freedom of the first zinc ligand residue, His 1, may be responsible for this structural variation, and supports the prediction of a helical structure at this region.

In our study, the peptide contains one tryptophan residue in β4 and this residue is located between β5 and α15, Figure 4b. We believe that when the zinc ion binds to the HEMGH and EAIG sites, the structural conformation of the molecule changes. Specifically, β4 is rotated toward the outside of the molecule because the zinc-binding sites are found in α15 and α17 of the HEMGH and EAIG, respectively. This conformational change was observed by the decrease in intensity that corresponds to the tryptophan exposition. When tryptophan is placed in a hydrophilic environment (exposed to solvent), the quantum yield of the amino acid decreases and leads to low florescence intensity [33]. Our cs-ACE_C analyses were made in Tris-HCl and NaCl buffer, which are both hydrophilic environments.

As far the activity of the peptide, this was analyzed by hydrolysis of the substrate Hip-His-Leu and the KM value obtained was 2.4 mM. The KM data obtained are similar to sACE results in Wistar rats [34] and humans [35] and recombinant human sACEC [27]. The affinity of ACE for the Hip-His-Leu substrate is variable (Table 3). This variation may be due to several factors, such as the use of cell or bacterial culture expression systems, the type of cell culture or expression vector, and the type of buffer used, including borate, phosphate or Tris-HCl [36].

Studies on the inhibition activity of ACEs show that there is a trend in the relative potencies of lisinopril, enalaprilat and captopril for the C-domain (L > E > C). This trend correlates with the number of interactions observed in the crystal structure complexes with tACE [28].

ACE Class	K_M (mM)	Origin	Reference
sACE	3.0*	Serum rat wistar	[37]
	1.1**		
Wild-type	1.54	Human recombinant (CHO)	[27]
C-fragment	2		
C-frag - D362	1.59		
C-frag - K361/365	1.59		
sCAE	2.3	Human	[35]
	5.8	Guinea pig	
sACE	1.6	Human recombinant CHO	[38]
C-Domain	1.5		
sACE	2	Rat wistar Culture medium	[34]
sACE	3	Mesangial cell	
sACE	3	Premature infants urine	[39]
sACE	0.9	Bovine	[31]
C-Domain	1.7	Human	[40]
sACE	3	Human Pericardial fluid	[41]
C-domain	3.5	Human	[42]
cs-ACE_C	2.4	Human recombinant	Current study

* 0.1 M Potassium phosphate with 0.3 M NaCl buffer

**0.4 M Sodium borate with 0.9 M NaCl buffer

Table 3. Kinetic parameters of ACE activity for the hydrolysis of Hip-His-Leu substrate using a Michaelis complex simulation.

Interactions with the inhibitor as indicated in Fig.1b, the phenyl ring of the lisinopril interacts with the probable S1 subsite in the active site, the lysine interacts with the S1' subsite and the proline occupies the S2' subsite. When the lisinopril is not bound, ACE cleaves the bond between residues of a substrate that occupy the S1 and S1' subsites [43].

The binding between the catalytic site ACEC and lisinopril occurs via the zinc ligands His383/988, His387/992, Glu411/1016 (tACE/cs-ACE$_C$), and the C4 carboxylate oxygen 1 (O1) of lisinopril or enalapril [44]. The low activity of the cs-ACE$_C$ in the presence of lisinopril, 59%, was also obtained by Andrade et al. [34,45], who reported values of 64% and 60% in Wistar and spontaneously hypertensive rats, respectively.

ACE inhibitors were the first drugs to be widely prescribed for the treatment of cardiovascular diseases. However, these inhibitors are not well-tolerated by 10-20% of patients due to the development of a persistent dry cough or angioedema (0.3%) [46]. These effects are likely caused by an increase in bradykinin levels. When the C-domain region of ACE was inactivated in a mutant mouse, the hydrolysis of Ang I and II was reduced, while the peptides (1-7) and (1-9) derived from bradykinin showed no significant changes. This experiment showed that inhibitors that bind only the C-domain can maintain bradykinin hydrolysis and blood pressure regulation [47,48]. In our study, the results with lisinopril were in agreement with the previously reported data.

Conclusion

In the present work, we have established an efficient protocol for obtaining the zinc catalytic site in the Ala^{959} to Ser^{1066} region of recombinant sACEC. The strategy for producing pure cs-ACE$_C$ in the correct structural conformation involves a single purification step. This result shows that recombinant cs-ACE$_C$ has an α-helix and β-strand structure, which zinc ion (essential for its activity) binds to cs-ACE$_C$, and in agreement with the results the enzymatic activity of the protein this was inhibited by lisinopril. Obtaining this cs-sACEC region in the correct structural conformation is critical for studying inhibitor binding, and our results provide a new approach to obtain the catalytic site region with activity, it facilitating the studies with novel inhibitors.

Acknowledgments

We thank Dr. Juliana Fattori from the Laboratório de Espectroscopia e Calorimetria - Pólo II de Alta Tecnologia (LNLS-SP) and the members of the Grupo de Hormônios from the Centro de Biotecnologia and the Centro de Química e Meio Ambiental IPEN/CNEN-SP. We also thank CNPq for financial support of the graduate student stipend.

The first two authors contributed equally to this work.

References

1. Andrade MCC, R Affonso, Fernandes FB, Febba AC, Silva ID et al. Spectroscopic and structural analysis of somatic and N-domain angiotensina I-converting enzyme isoforms from mesangial cells from Wistar and spontaneously hypertensive rats. Int. J. Biol. Macromol. 2010, 47(2): 238-243.

2. Anthony CS, Masuyer G, Sturrock ED, Acharya KR. Structure Based Drug Design of Angiotensin-I Converting Enzyme Inhibitors. Curr. Med. Chem. 2012, 19(6): 845-855.

3. Elisseeva YE, Kugaevskaya EV. Structure and Physiological Importance of Angiotensin Converting Enzyme Domains. Biochemistry (Moscow). 2009, 3: 237-247.

4. Acharya KR, Sturrock ED, Riordan JF, Ehlers MR. ACE revisited: a new target for Structure-based drug design. Nat. Rev. Drug. Discov. 2003, 2(11): 891-902.

5. Ferreira SH, Bartelt DC, Greene LJ. Isolation of bradykinin-potentiating peptides from Bothrops jararaca venom. Biochemistry. 1970, 9(13): 2583-2593.

6. Ondetti MA, Williams NJ, Sabo EF, Pluscec J, Weaver ER et al. Angiotensin-converting enzyme inhibitors from the venom of Bothrops jararaca. Isolation, elucidation of structure, and synthesis. Biochemistry J. Renin Angiotensin Aldosterone Syst. 1971, 10(22): 4033-4039.

7. Spyroulias GA, Galanis AS, Pairas G, Manessi-Zoupa E, Cordopatis P. Structural features of angiotensin-I converting enzyme catalytic sites: conformational studies in solution, homology models and comparison with other zinc metallopeptidases. Curr. Top. Med. Chem. 2004, 4(4): 403-429.

8. Galanis AS, Spyroulias GA, Pairas G, Manessi-Zoupa E, Cordopatis P. Solid-phase synthesis and conformational properties of angiotensin converting enzyme catalytic-site peptides: the basis for a structural study on the enzyme-substrate interaction. Biopolymers. 2004, 76(6): 512-526.

9. Vamvakas SS, Leondiadis ML, Pairas, G Manes E, Cordopatis P. Expression, purification, and physicochemical characterization of the N-terminal active site of human angiotensin-I converting enzyme. J. Pept. Sci. 2007, 13(1): 31-36.

10. Vamvakas SS, Leondiadis ML, Pairas, G Manes E, Cordopatis P. Folding in solution of the C-catalytic protein fragment of angiotensin-converting enzyme. J. Pept. Sci. 2009, 15(8): 504-510.

11. Spyranti Z, Galanis AS, Pairas G, Spyroulias GA, Manessi-Zoupa E. Synthetic Peptides as Structural Maquettes of An-

giotensin-I Converting Enzyme Catalytic Sites. Bioinorg. Chem. Appl. 2010, 1-13.

12. Guang C, Phillips RD, Jiang B, Milani F. Three key proteases--angiotensin-I-converting enzyme (ACE), ACE2 and renin--within and beyond the renin-angiotensin system. Arch. Cardiovasc. Dis. 2012, 105(6-7): 373-385.

13. Sørensen HP, Mortensen KK. Advanced genetic strategies for recombinant protein expression in Escherichia coli. J. Biotechnol. 2005, 115(2): 113-128.

14. Yin J, Li G, Ren X, Herrler G. Select what you need: A comparative evaluation of the advantages and limitations of frequently used expression systems for foreign genes. J. Biotechnol. 2007, 127(3): 335-347.

15. Carvalho CV, Ricci G, Affonso R. Guia de praticas em Biologia Molecular, second ed., Yends, São Paulo, Br, 2015.

16. Pereira LM, Silva LR, Alves JF, Marin N, Silva FS et al. A simple strategy for the purification of native recombinant full-length human RPL10 protein from inclusion bodies. Protein Expres. Purif. 2014, 101:115-120.

17. Laemmli UK. Cleavage of structure proteins during the assembly of the head of bacteriophage T4. Nature. 1970, 227(5259): 680-685.

18. Callaway D. Beer-Lambert L. J Chem. Educ. 1997, 74: 737-871.

19. Bohm G, Muhr R, Jaenicke R. Quantitative analysis of protein far UV circular dichroism spectra by neural networks. Protein Eng. 1992, 5(3): 191-195.

20. Friedland J, Silverstein E. A sensitive fluorometric assay for serum angiotensin converting enzyme. Am. J. Clin. Pathol. 1976, 66(2): 416-424.

21. Marques GD, Quinto BM, Plavnik FL, Krieger JE, Marson O et al. N-domain angiotensin I-converting enzyme with 80 kDa as a possible genetic marker of hypertension. Hypertension. 2003, 42(4): 693-701.

22. Ehlers MR, Abrie JA, Sturrock ED. C domain-selective inhibition of angiotensin-converting enzyme. J. Renin Angiotensin Aldosterone Syst. 2013, 14(2): 189-192.

23. Hansted JG, Pietikäinen L, Hög F, Sperling-Petersen HU, Mortensen KK. Expressivity tag: A novel tool for increased expression in Escherichia coli. J. Biotechnol. 2011: 155(3):275-283.

24. Rosano GL, Ceccarelli EA. Recombinant protein expression in Escherichia coli: advances and challenges. Front Microbiol. 2014, 5: 1-17.

25. Kelly S, Jess TJ, Price NC. How to study proteins by circular dichroism, Biochim. Biophys. Acta. 2005, 1751(2): 119-139.

26. Corradi HR, Schwager SLU, Nchinda AT, Sturrock ED, Acharya KR. Crystal structure of the N domain of human somatic angiotensina I-converting enzyme provides a structural basis for domain-specific inhibitor design. J.Mol. Biol. 2006, 357(3): 964-974.

27. Wei L, Clauser E, Alhenc-Gelas F, Corvol P. The two homologous domains of human angiotensin I-converting enzyme interact differently with competitive inhibitors. J. Biol. Chem. 1992, 267(19): 13398-13405.

28. Anthony CS, Corradi HR, Schwager SLU, Redelinghuys P, Georgiadis D et al. The N domain of human angiotensin-I converting enzyme: the role of N-glycosylation and the crystal structure in complex with an N domain specific phosphinic inhibitor RXP407. J. Biol. Chem. 2010, 285(46): 35685-35693.

29. Peternel S, Grdadolnik J, Gaberc-Porekar V, Komel R. Engineering inclusion bodies for non denaturing extraction of functional proteins. Microb. Cell Fact. 2008, 7: 34.

30. Ikeguchi M. Transient Non-Native Helix Formation during the Folding of beta-Lactoglobulin. Biomolecules. 2014, 4(1): 202-216.

31. Voronov S, Zueva N, Orlov V, Arutyunyan A, Kost O. Temperature induced selective death of the C-domain within angiotensina converting enzyme molecule. FEBS Lett. 2002, 522(1-3): 77-82.

32. Borden KLB. Ring fingers and B-boxes: Zinc-binding protein-protein interaction domains Biochem. Cell Biol. 1998, 76(2-3): 351-358.

33. Lakowicz JR. Principles of Fluorescence Spectroscopy, third ed., Springer, US, 2006.

34. Andrade MCC, Quinto BMR, Carmona AK, Ribas OS, Boim MA et al. Purification and characterization of angiotensin I-converting enzymes from mesangial cells in culture. Hypertension. 1998, 16(12 pt 2): 2063-2074.

35. Casarini DE, Carmona AK, Plavink FL, Zanella MT, Juliano L. Calcium channel blockers as inhibitors of angiotensin I-converting enzyme. Hypertension. 1995, 26(6 pt 2): 1145-1148.

36. Schomburg KT, Ardao I, Götz K, Rieckenberg F, Liese A et al. Computational biotechnology: Prediction of competitive substrate inhibition of enzymes by buffer compounds with pro-

tein–ligand docking. J. Biotechnol. 2012, 161(4): 391-401.

37. Santos RA, Krieger EM, Greene LJ. An improved fluorometric assay of rat serum and plasma converting enzyme. Hypertension. 1985, 7(2): 244-252.

38. Williams TA, Danilov S, Alhenc-Gelas F, Soubrier F. A study of chimeras constructed with the two domains of angiotensin I-converting enzyme. Biochem. Pharmacol. 1996, 51(1): 11-14.

39. Hattori MA, Del Ben GL, Carmona AK. Angiotensin I-converting enzyme isoforms (high and low molecular weight) in urine of premature and full-term infants. Hypertension. 2000, 35(6): 1284-1290.

40. Skirgello OE, Binevski PV, Pozdnev VF, Kost OA. Kinetic probes for inter-domain co-operation in human somatic angiotensin-converting enzyme. J. Biochem. 2005, 391(pt 3): 641-647.

41. Gomes RAS, Teodoro LGVL, Lopes ICR, Bersanetti PA, Carmona AK et al. Enzima Conversora de Angiotensina no Líquido Pericárdico: Estudo Comparativo com a Atividade Sérica. Arq Bras Cardiol. 2008, 91(3): 156-161.

42. Masuyer G, Schwager SLU, Sturrock ED, Isaac RE, Acharya KR. Molecular recognition and regulation of human angiotensin-I converting enzyme (ACE) activity by natural inhibitory peptides. Sci Rep. 2012, 2: 717.

43. Brew K. Structure of human ACE gives new insights into inhibitor binding and design. Trends Pharmacol Sc. 2003, 24(8): 391-394.

44. Wang X, Wu S, Xu D, Xie D, Guo H. Inhibitor and Substrate Binding by Angiotensin-converting Enzyme: Quantum Mechanical/Molecular Mechanical Molecular Dynamics Studies. J. Chem. Inf. Model. 2011, 51(5): 1074-1082.

45. Andrade MCC, Di Marco GS, Teixeira VPC, Mortara RA, Sabatini RA et al. Expression and localization of N-domain ANG I-converting enzymes in mesangial cells in culture from spontaneously hypertensive rats rats. Am J. Physiol. Renal. Physiol. 2006, 290(2): 364-375.

46. Denti P, Sharp SK, Kröger WL, Schwager SL, Mahajan A et al. Pharmacokinetic evaluation of lisinopril-tryptophan, a novel C-domain ACE inhibitor. Eur. J. Pharm. Sci. 2014, 56: 113-119.

47. Fuchs S, Xiao HD, Hubert C, Michaud A, Campbell DJ et al. Angiotensin-converting enzyme C-terminal catalytic domain is the main site of angiotensin I cleavage *in vivo*. Hypertension. 2008, 51(2): 267-274.

48. Lunow D, Kaiser S, Rückriemen J, Pohl C, Henle T. Tryptophan-containing dipeptides are C-domain selective inhibitors of angiotensin converting enzyme. Food Chem. 2015, 166: 596-602.